

**Paper No.**  
16751



## **Methodology of Batch Inhibition Applied for Top and Bottom of the Line Corrosion Mitigation**

Mengqiu Pan, Maryam Eslami, Yuan Ding, Zineb Belarbi, David Young, Marc Singer  
Institute of for Corrosion and Multiphase Technology  
Ohio University  
342 West State Street  
Athens, OH 45701

### **ABSTRACT**

Quaternary ammonium compounds that exist as a waxy solid at low temperatures typically exhibit excellent persistency when applied in batch corrosion inhibitors (BCI), which are one of the mainstays of corrosion protection for many integrity management strategies worldwide. The performance of these type of corrosion inhibitor is often evaluated in laboratory conditions, prior to field application. The most common laboratory method to characterize BCI involves the filming procedure called the dip and drip method, where the steel specimen is immersed in neat BCI for a few seconds before testing. However, this dip and drip method carries several drawbacks, one of them being the likely oxygen ( $O_2$ ) contamination what is sure to impact the results. In addition, extrapolation of laboratory measurements to field conditions are often performed without rigorous modeling, and application parameters are consequently suboptimal; this results in inefficient or, at worst, ineffective protection being provided to the steel in the corrosive environment. In this research, a BCI testing procedure was developed for bottom of the line corrosion (BLC) that can maintain stable water chemistry and avoid  $O_2$  contamination, with the potential to be adapted for top-of-the-line corrosion (TLC) environments. The pre-filming procedure of BCI and corrosion testing can be done in the same glass cell which eliminates  $O_2$  contamination and have capabilities to remove residual inhibitors after the pre-filming process. The linear polarization resistance (LPR) method was utilized to measure in situ corrosion rates. UV-vis spectroscopy was applied to monitor corrosion inhibitor concentrations, which showed repeatable results and demonstrated the accuracy and efficiency of this methodology of batch inhibition applied for BLC and TLC mitigation.

Key words: Batch inhibition, mild steel, TLC mitigation, inhibitor concentration

### **INTRODUCTION**

Corrosion leads to economic costs equivalent to 4-5% of gross national product (GNP), environmental contamination, infrastructure degradation, safety risks, reputational damage, and litigation <sup>1</sup>. However, 35% of the cost of corrosion can be reduced by adoption of appropriate mitigation measures <sup>2</sup>. In the industry of transportation of oil and gas, much effort has been made to understand the role of  $CO_2$  in internal corrosion of pipelines, due to the ubiquitous presence of the corrosive gas in wells and geologic formations <sup>3-8</sup>. Main mitigation strategies include use of coatings, cathodic protection, corrosion resistant alloys, and organic corrosion inhibitors. The use of corrosion inhibitor presents many advantages for internal corrosion. First, inhibitors can be directly injected in the flow without affecting

production and their use are relatively versatile as injection rates can be adjusted easily <sup>9</sup>. Secondly and most importantly, its associated costs are low compared to other mitigation techniques <sup>9</sup>.

Batch corrosion inhibitors are among common methods of protection against bottom-of-the-line corrosion (BLC) and top-of-the-line corrosion (TLC). These inhibitors are usually high molecular-weight and oil-soluble molecules. Such materials are tenacious, sticking well to pipe surfaces <sup>10</sup>. However, mature oil and gas wells generate large amounts of water. Consequently, water dispersible inhibitors are applied in such production environments. The difference in most batch corrosion inhibitors usually is their formulation, i.e., which molecular species are present therein.

The standard filming procedure for inhibitor evaluation is called the dip and drip method. In this method, mild steel specimens are first polished to a certain (600 or 800 grit) finish. They are then dipped into an inhibitor solution for a specified period at room temperature. During this process, the contact time varies and might affect the persistency <sup>11</sup>. The specimen is then drip dried (25 minutes to 1 hour) <sup>11</sup>. Excess inhibitor might be wiped from the specimens <sup>11</sup>. In addition, there may be a “rinse step” with a model brine <sup>12</sup>. In each step of the procedure, it is likely that O<sub>2</sub> contamination will impact the results.

So far, accurate modeling of batch corrosion inhibitor application for BLC and TLC has not been performed. Moreover, application parameters have not been optimized, which results in inefficient, or ineffective, corrosion protection.

Considering this gap in knowledge and practice, this research aimed to improve the testing/treatment protocol for BCI and its applicability to BLC and TLC scenarios.

## EXPERIMENTAL PROCEDURE

### Tested Inhibitor in BLC and TLC Experiments

BCI formulations used in industry are typically a proprietary cocktail of several molecules, some acting as the actual corrosion inhibitors and others to aid dispersion. However, for a mechanistic study, it is better to study one single compound. The choice of this model compound is somehow arbitrary, as long as it is representative, and its composition is known. The ICMT has a long history of synthesizing and characterizing model CIs, especially quaternary ammonium-type chemical products <sup>13</sup>. The efficiency of batch corrosion inhibitors is typically related to the alkyl tail length <sup>13</sup>. For this study, the model compound benzyldimethylhexadecyl ammonium (C16-BDA) (Figure 1) was chosen as the inhibitor to investigate the application of BCI to BLC and TLC. While the head group is quaternary ammonium-type, the choice of the tail length (C16-BDA) was made based on preliminary data that showed superior performances <sup>13</sup>. The surface saturation concentration of C16-BDA was set at 50ppm<sub>w</sub> in 1 wt.% NaCl solution<sup>13</sup>. C16-BDA is synthesized in-house as a waxy solid and needs to be solubilized in isopropanol before injection. To simulate batch treatment, 1 mL of a deoxygenated isopropanol solution with 15 wt% inhibitor was sprayed on the API 5L X65 mild steel specimen surface. Assuming full dissolution in the testing electrolyte, the corresponding inhibitor concentration should be 75 ppm<sub>w</sub>.

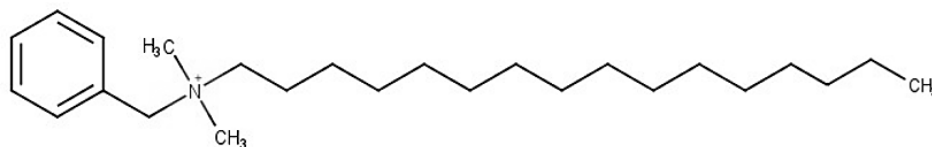


**Figure 1 Benzyldimethylhexadecyl ammonium (C16-BDA) molecule**

## Batch Treatment Testing Protocol for BLC

Experiments were conducted using the “controlled water chemistry” glass cell setup as shown in Figure 2.

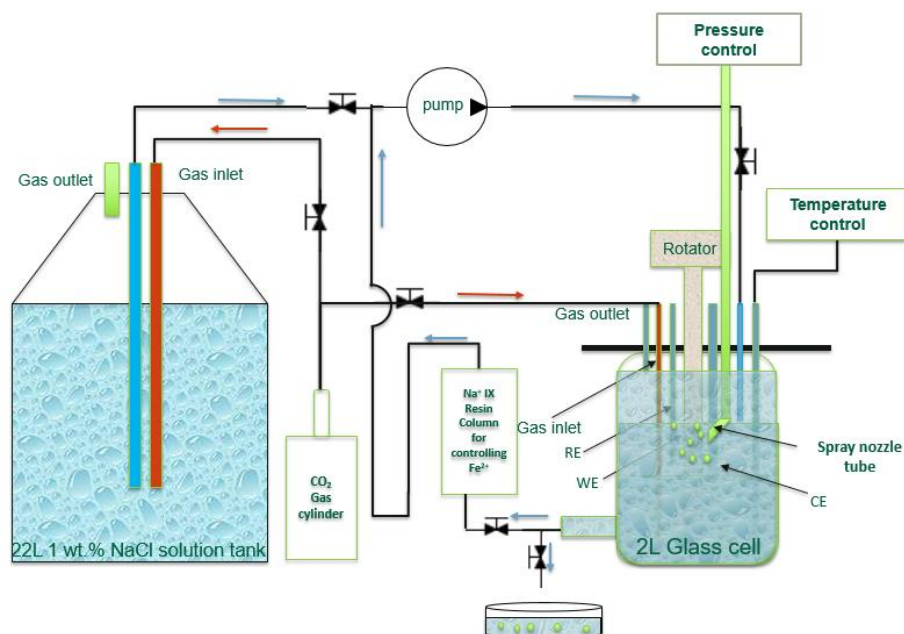


**Figure 2 Schematic representation of the experimental setup for batch treatment testing**

Four steps were required to begin the corrosion testing. It started with the inhibitor solution formulation and deoxygenation. A 15 wt% C16-BDA solution was prepared by dissolving the inhibitor in isopropanol. The inhibitor solution was then deoxygenated with nitrogen (N<sub>2</sub>) for 2 hours. Then 22 L of 1 wt% sodium chloride (NaCl) electrolyte was purged with carbon dioxide (CO<sub>2</sub>) for 6 hours to assure that all the dissolved oxygen was removed, and the solution was saturated with CO<sub>2</sub>. A magnetic stirrer was used to ensure that the solution was always well mixed. A Na<sup>+</sup>-form ion exchange resin (Amberlite, IR120, Acros Organics) was used to control Fe<sup>2+</sup> concentration ([Fe<sup>2+</sup>]). The electrolyte pH was controlled manually controlled at around pH 4 using dilute hydrochloric acid (HCl) or sodium bicarbonate (NaHCO<sub>3</sub>) solutions. The resins were added into the columns and purged with CO<sub>2</sub> for 2 hours.

The steel specimens used in this part of the study were standard rotating cylinder electrode (RCE). The specimens were sequentially polished with silicon carbide paper of 150, 400, 600 grit. They were then sonicated in isopropanol to remove any residual particles or contamination and dried with N<sub>2</sub>. The surface area of each specimen was measured.

After these initial steps were completed, the glass cell was assembled as shown in Figure 2. The working electrode was then installed, and the glass cell was purged with CO<sub>2</sub> for 2 hours. As for the final step, the glass cell and the purged columns with ion-exchange resins were put together with continuous CO<sub>2</sub> purging until the start of solution transfer.

When the system was properly purged, the desired volume (1mL) of the deoxygenated inhibitor was injected into the tubing connected to the nozzle. The tubing was then pressurized with CO<sub>2</sub> (pCO<sub>2</sub>~30 psi). At this point, the rotation of the cylinder was started at a 200rpm rate and the valve connected to the inhibitor injection nozzle was opened to create a mist that was applied to the entire surface of the

specimen. After 30 seconds of inhibitor spraying, the pre-purged electrolyte was pumped into the glass cell at the rate of 2000 mL/min. The pumping was stopped after the solution volume in the glass cell reached 2 L, ensuring that the specimen was fully immersed in the electrolyte. This procedure was repeated 7 times. It is noteworthy that foaming occurred during this procedure but that the amount of foam at the water/air interface decreased after each rinse, suggesting that less inhibitor remained in the test solution.

After the rinsing step was completed, the loop with Na<sup>+</sup>-exchanged resins was opened to circulate the solution. Linear polarization resistance measurements were conducted using a traditional three electrode set up and a Gamry potentiostat. The Stern Geary equation was used to convert the polarization resistance into a corrosion rate, using a B value 26mv/dec<sup>14</sup>. A saturated silver/silver chloride Ag/AgCl (KCl sat) reference electrode and a platinum counter electrode were used for the electrochemical experiments. Table 1 shows the experimental matrix that was followed to examine the corrosion persistency of the batch inhibitor.

**Table 1 Test matrix for the BLC electrochemical experiment**

Parameter	Conditions
CO <sub>2</sub> partial pressure	0.96 bar
Solution	1 wt.% deoxygenated NaCl solution
Inhibitor solution	15 wt.% C16-BDA
pH	4.00 ± 0.02
Temperature	30.0°C
RCE rotation speed	1000 rpm
Material	API 5L X65 mild steel
Corrosion Rate Measurement	LPR, weight loss

### Batch Treatment Testing Protocol for TLC

The schematic of the experimental setup for TLC mitigation experiments is shown in Figure 3. This setup is similar to what was used for the BLC scenario. The main differences lie in the steel samples location (in TLC experiments they are flushed to the top lid and exposed to the vapor phase), the method of Cl injection (sprayed in a fine mist on the specimen surface) and the corrosion measurement method (weight loss and ferrous ion [Fe<sup>2+</sup>] measurement).

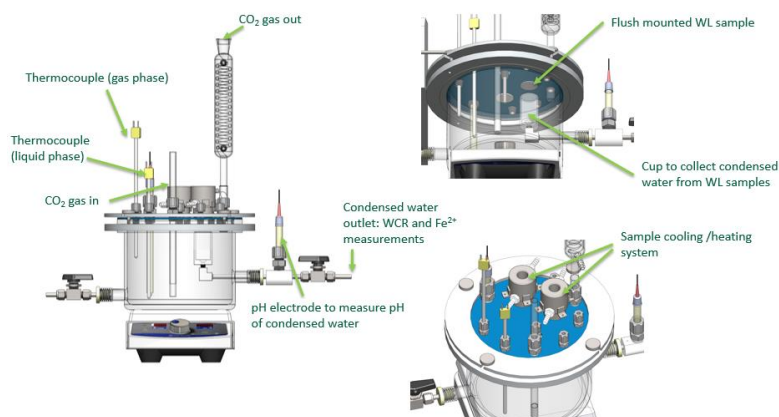


**Figure 3 Schematic of the experimental setup for TLC (Image courtesy of Cody Shafer, ICMT)**

In these experiments, 1 mL of deoxygenated 15 wt.% C16-BDA (dissolved in isopropanol, 75 ppm<sub>w</sub> total) was sprayed on the surface of X65 mild steel specimen using the spray nozzle as shown in Figure 4.



**Figure 4 Inhibitor spray nozzle for TLC experiment**

Table 2 shows the experimental matrix that was followed to test the persistency of the batch corrosion inhibitor in TLC experiments. A set relatively aggressive conditions were selected, featuring high temperature and water condensation rate, to verify the applicability of batch treatment to TLC and to evaluate the persistency of BCI in condensing environment.

**Table 2 Test matrix for the TLC experiment**

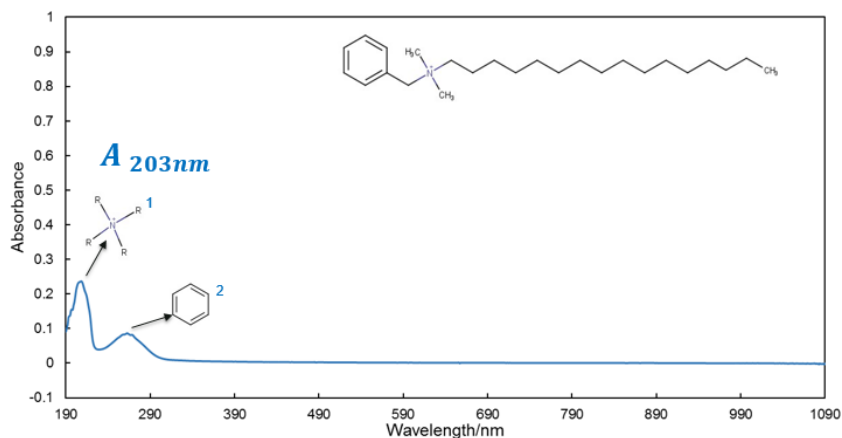
Parameter	Conditions
<b>CO<sub>2</sub> partial pressure</b>	0.96 bar
<b>Solution</b>	Deionized water
<b>Inhibitor solution</b>	15 wt.% C16-BDA
<b>pH of the bulk electrolyte</b>	4.00 ± 0.02
<b>Steel temperature</b>	35.5 °C
<b>Liquid temperature</b>	75.0 °C
<b>Gas temperature</b>	65.0 °C
<b>Magnetic stirrer rotation speed</b>	200 rpm
<b>Materials</b>	API 5L X65 mild steel, 304 stainless steel
<b>Corrosion Rate Measurements</b>	Ferrous ion concentration measurement Weight loss specimen
<b>Water condensation rate</b>	1.4 mL/(m <sup>2</sup> ·s)

## RESULTS AND DISCUSSION

### Inhibitor Concentration Monitoring

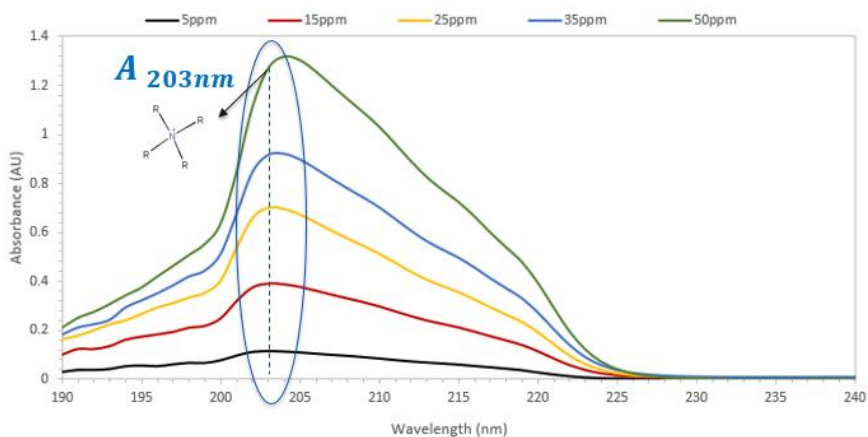
UV-Vis measurements were performed to monitor the concentration of inhibitor in the glass cell solution during the corrosion rate measurements. It was expected that the inhibitor would continuously desorb from the steel sample even after the rinsing steps. A calibration curve of C16-BDA was generated by measuring absorbance at different concentrations. UV-Vis absorbance measurements were performed using an Agilent Cary 60 UV-Vis spectrometer.

Figure 5 shows the UV-vis spectrum of C16-BDA. The peaks at 203 nm and 268 nm wavelengths labeled as 1 and 2 are related to quaternary ammonium group and benzene ring of the C16-BDA, respectively. In the molecule, the nitrogen atom is the main adsorption site. The peak at the wavelength of 203 nm was selected for calibration and C16-BDA concentration measurements.



**Figure 5 UV Spectrum of C16-BDA**

Figure 6 presents the UV-vis spectra obtained for different concentrations of C16-BDA dissolved in 1 wt.% NaCl electrolyte. At the wavelength of 203 nm, the absorbance peak increases with the inhibitor concentration.



**Figure 6 UV Spectra for different concentrations of C16-BDA in 1 wt% NaCl electrolyte**

The calibration curve obtained from the UV-vis measurements is presented in Figure 7. The Beer-Lambert law equation<sup>15</sup> was used to relate the absorbance to the concentration of C16-BDA in the solution:

$$A = \epsilon bC \quad (1)$$

In Equation (1),  $A$  is the absorbance (a.u.),  $\epsilon$  is the molar absorptivity (L/mol.cm),  $b$  is the path length (cm), and  $C$  is the concentration (mol/L).

The UV-vis measurement at each concentration (in a range of 0 ppm to 60 ppm) was repeated 5 times. As observed in Figure 7, the obtained curve shows an excellent linearity ( $R^2 = 0.9924$ ). The inhibitor

concentration in the solution can then be calculated from absorbance measurements and the calibration curve.

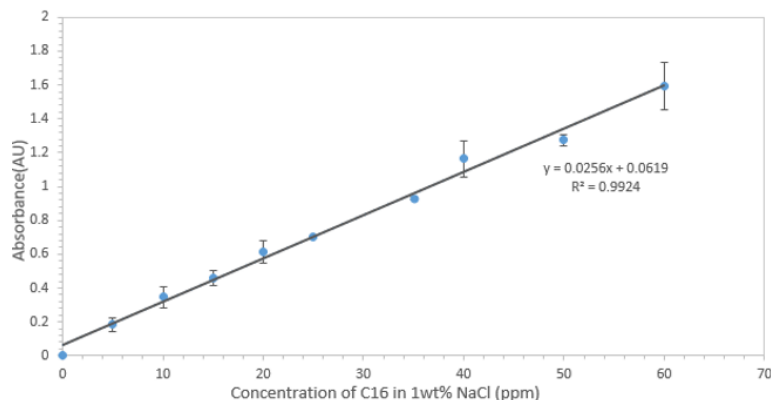


**Figure 7 The absorbance calibration curve for C16-BDA in 1 wt% NaCl aqueous solution.**

The UV-vis absorbance curves obtained in the 1 wt% NaCl aqueous solutions after the 7 to 9 rinsing steps (but before the start of the electrochemical measurements) are shown in Figure 8. The collected spectra in these cases do not present any peak at 203 nm. This means that the rinse procedure in the BLC experiments can remove all the inhibitor left in the glass cell after the filming process.

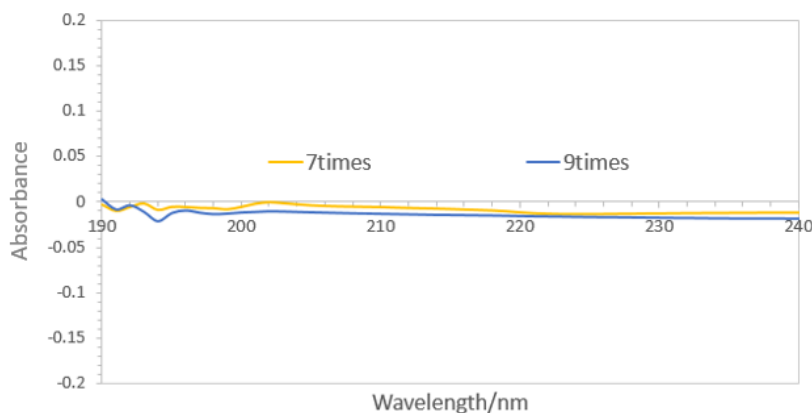


**Figure 8 UV spectra of rinsed glass cell solutions (7<sup>th</sup> and 9<sup>th</sup> rinse).**

### BLC Corrosion Rate Analysis

Figure 9 shows the corrosion rate without the inhibitor (the blank test) and after exposure to the batch treatment. It should be noted that the aforementioned figure presents results of repetitions of the same experiment. According to Figure 9, in the absence of the batch treatment inhibitor, the corrosion rate remained constant at around 3.5 mm/y during the entire measurement. However, with the application of batch corrosion inhibitor C16-BDA and its subsequent removal by rinsing, the corrosion rate was decreased to around 0.5 mm/y immediately after the rinsing procedure (time 0 hour) and remained constant for approximately 20 hours. The corrosion rate increased progressively to reach a value of around 2.9 mm/year after 60 hours of exposure and remained relatively stable until 90 hours. The BCI showed a relatively long persistency (50 to 60 hours). However, the corrosion resistance started to decrease only after 20 hours of exposure. From these figures, it is clear that the OCP of the sample shifted to more anodic potential after exposure to BCI (at the beginning of the experiments) compared to the blank. This confirmed that the inhibitor initially quickly adsorbed on the sample surface and, with

time, slowly desorbed, as shown by the gradual decrease in OCP which eventually reached the same value as the blank. However, the timeline of change in OCP does not follow exactly the change in corrosion rate. Since both processes are directly dependent on the Cl adsorption/desorption equilibrium, some correspondence was expected (i.e. the OCP shift should have occurred around the same time as the loss of inhibition efficiency). While the reason behind this discrepancy must be related to the desorption of BCI and the change in surface coverage of inhibitor on the sample surface<sup>13</sup>, a comprehensive mechanistic explanation is still elusive at this point. Data depicted in trial 1 (Figure 9 [a]) and trial 2 (Figure 9 [b]) show good repeatability.

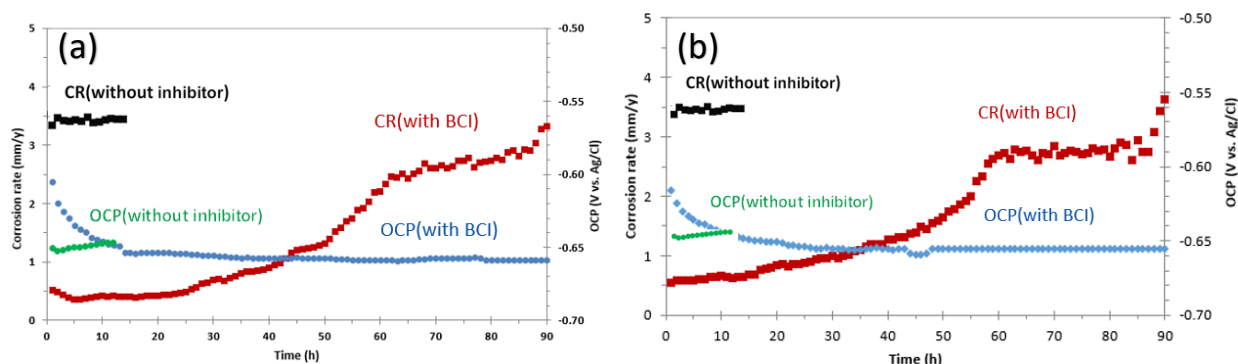


**Figure 9 Corrosion rate versus time: (a) Trial 1 and (b) Trial 2 (the experimental conditions for both trials: T 30°C, pH 4.0,  $\omega$ =1000 rpm, 0.96 bar CO<sub>2</sub>)**

During the electrochemical measurements, 5 ml (each time) of the NaCl electrolyte was retrieved regularly from the glass cell for UV absorbance measurements to monitor the inhibitor concentration. Based on the absorbance peak of solution samples and the calibration curve of the C16-BDA in NaCl solutions, the inhibitor concentration in solution samples was calculated and is shown in Figure 10.

In experiment 1 (Figure 9 [a]), at the beginning of the experiment (after the rinses), the concentration of inhibitor in the glass cell solution was 0 ppm. After 15 and 55 hours of exposure, the inhibitor concentration increased to 3.4 ppm and 18.6 ppm, respectively. The final concentration of C16-BDA in the glass cell solution at the end of this experiment (87 hours) reached 26.4 ppm. In experiment 2 (Figure 9 [b]), at the beginning of the experiment, the concentration of inhibitor in the glass cell solution was 0 ppm. The inhibitor concentration in the glass cell solution gradually increased with the exposure time.

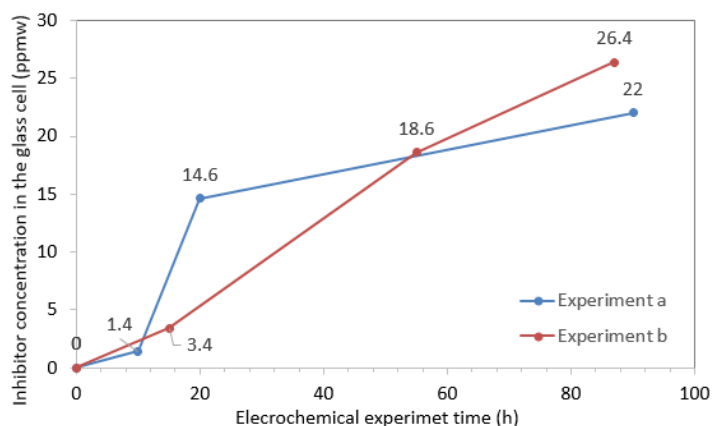


**Figure 10 Inhibitor concentration in the glass cell solution versus time (experimental conditions for a and b: T 30°C, pH 4.0,  $\omega$ =1000 rpm, 0.96 bar CO<sub>2</sub>)**

It is hypothesized that the inhibitor that was initially adsorbed on the metal specimen surface (and all other possible surfaces in the glass cell) was slowly desorbed. At the beginning of the experiments, a thick layer of inhibitor formed on the sample surface by the spray filming procedure. While some CI was removed by the rinsing procedure, the corrosion rate results show that a CI film remained on the metal surface. The surface coverage of inhibitor on the sample surface, initially at its maximum value, slowly decreased after 20 hours of exposure via the desorption process<sup>13</sup>. This means that the inhibitor was continually released from the specimen surface, leading to the increase of the corrosion rate, but also leading to an increase in CI concentration in the aqueous solution. The surface saturation concentration of C16-BDA was previously determined at 50 ppm<sub>w</sub> in 1 wt.% NaCl solution<sup>13</sup>. Since the concentration of inhibitor at the end of the experiment (90 hours) was 26ppm<sub>w</sub>, it was expected that the final corrosion rate would not fully return to its baseline (un-inhibited) value.

## TLC Rate Analysis

The TLC corrosion rate was calculated based on the Fe<sup>2+</sup> concentration measurement in the condensed water. The results are presented in Figure 11 for two separate experiments under the same experimental conditions.

According to Figure 11, the corrosion rate of the blank specimen without BCI treatment remained at 0.4 mm/y (trial 1 [Figure 11(a)]) and 0.6 mm/y (trial 2 [Figure 11(b)]) for 55 hours of the experiment (black squares). The corrosion rate of the BCI treated specimen was 0.02 mm/y at the beginning of the experiment and remained at 0.04 mm/y for 30 hours, after which it increased to 0.2 mm/y over the remaining time of the exposure (red dots).

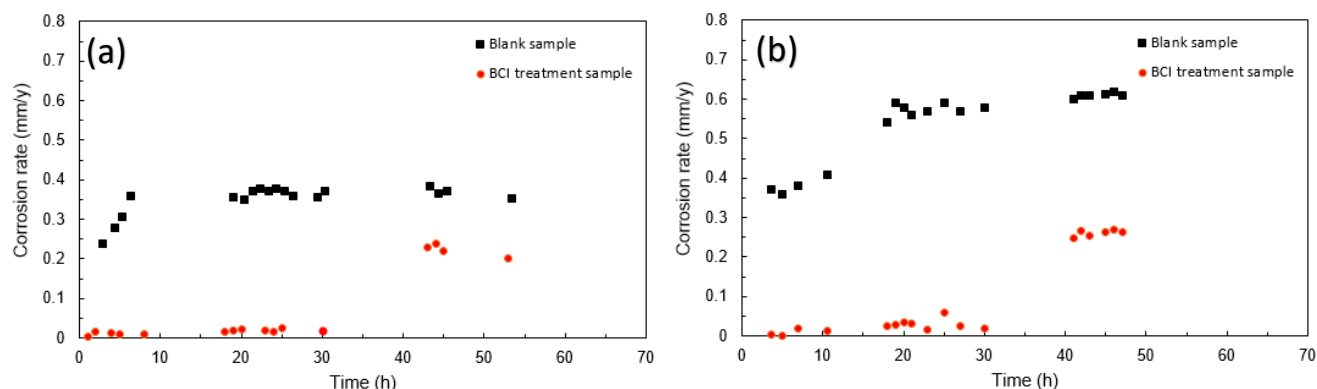


**Figure 11 TLC rate based on Fe<sup>2+</sup> concentration measurements in the condensed water: (a) Trial 1 and (b) Trial 2 (the experimental conditions for both trials: T<sub>gas</sub> 65°C, T<sub>specimen</sub> 35.5°C, pCO<sub>2</sub> 0.65 bar)**

From weight loss measurements, the corrosion rate of the blank specimen was around 0.7 mm/y and for the BCI treated specimen it was 0.3 mm/y, which represents an average mass loss rate over the periods of effective inhibition (first 40 hours) and of loss of persistency (last 15 hours). Looking at the visual images of the two specimens (Figure 12), there was basically not much difference in their appearance. Figure 13 (a) and (b) shows the SEM and EDS analysis of the specimens exposed to the TLC experiments with and without batch treatment before removing the corrosion product. Iron carbide covered on the both surfaces uniformly. Figure 13 (c) and (d) depicts the same analysis on the same specimens after removing the corrosion product layer. As can be seen in Figure 13, there was little difference between the morphology and the chemical composition of corrosion products and general corrosion was observed in both cases and no localized corrosion was detected.

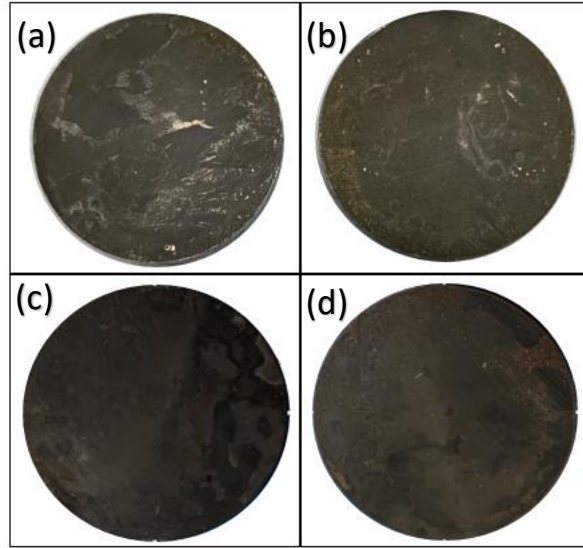


**Figure 12 Visual images of the specimens subjected to TLC experiments: (a) blank specimen (trial 1, Figure 11 [a]), (b) BCI treated specimen (trial 1, Figure 11 [a]), (c) blank specimen (trial 2, Figure 11 [b]), and (d) BCI treated specimen (trial 2, Figure 11 [b])**

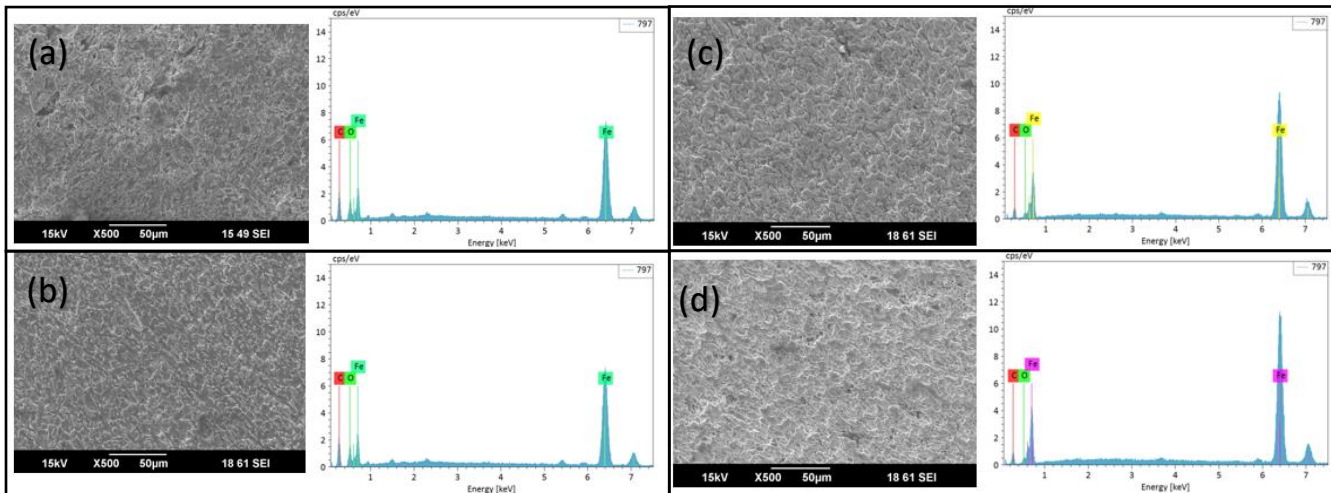


**Figure 13 SEM-EDS analysis of the specimen subjected to TLC experiment: (a) surface of the blank specimen, (b) surface of the BCI treated specimen, (c) surface of the blank specimen after removing the corrosion products, (d) surface of BCI treated specimen after removing the corrosion products (results are related to trial 1, Figure 11 [a]).**

### Monitoring of Inhibitor Concentration during the TLC Experiments

Figure 14 shows the UV-vis spectra of the condensed water recovered with time. The peak corresponding to C16-BDA's quat-type structural moiety at wavelength 203 nm shows considerable shifting. It is postulated that concentration of inhibitor could not be measured accurately by UV-vis due to the influence of  $\text{Fe}^{2+}$  in the condensed water, resulting from the corrosion of the steel specimen on the UV-vis spectrum. It is important to mention that the same problem was not encountered in the BLC experiments because of the  $\text{Na}^+$ -form ion exchange resin that was used to control  $\text{Fe}^{2+}$  concentration.

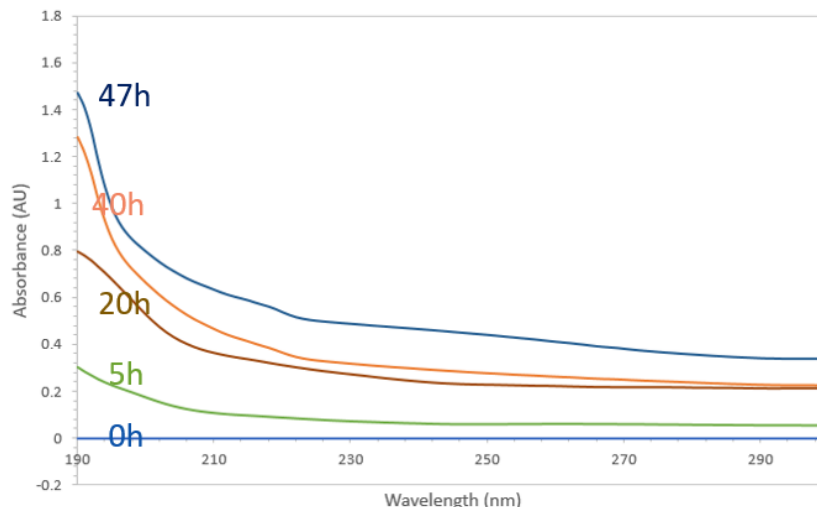


**Figure 14 UV Spectra of the condensed water recovered during the TLC experiment.**

To measure the inhibitor concentration during the TLC experiments, the same experimental set up as before was used (Figure 3) except that the X65 steel specimen was replaced with a 304 stainless steel to avoid the presence and influence of  $Fe^{2+}$  on the UV absorbance measurements. The TLC experiment was repeated under the same conditions as stated previously. The loss of the corrosion inhibitor from the specimen surface with the exposure time was then measured by UV-vis spectroscopy. The 304 stainless steel being corrosion resistance, no  $Fe^{2+}$  ion was released in solution. It was also assumed that the Cl adsorption/desorption process on API-X65 and SS-304 are similar.

Figure 15 shows the UV-vis spectra of the condensed water within 2 days when the X65 steel specimen was replaced with a 304 stainless steel. The absorbance peak at 203 nm increases with time.

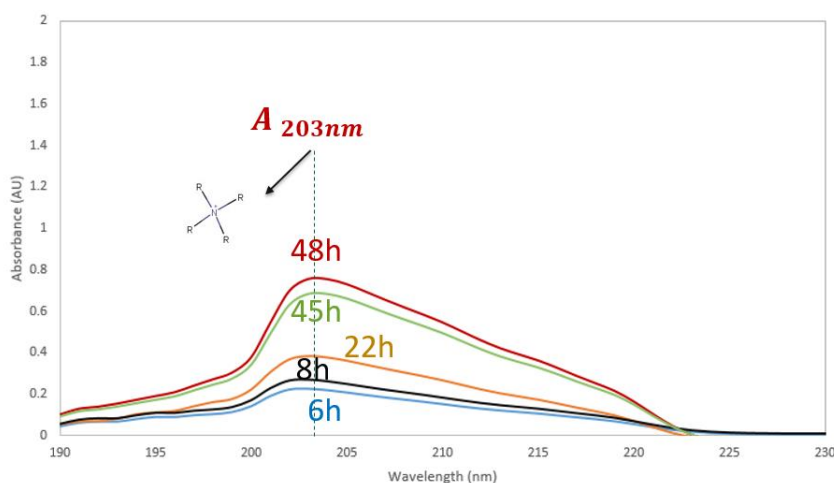


**Figure 15 UV Spectra of the condensed water recovered during the TLC experiment with stainless steel as TLC specimen.**

From the absorbance value and the inhibitor calibration curve, the CI concentration in the bottom solution can be calculated and is shown to increase with time at a rate of 0.63 ppm/h. Based on the 2L glass cell solution and on the surface area of the steel specimen, this corresponds to a rate of Cl desorption from the sample surface of 1.26mg/h.

Figure 16 shows a schematic representation of the way the inhibitor desorbed from the metal surface and dissolved in the condensed droplets (a) and how the inhibitor covered the metal surface immediately after it was applied (b). The diameter of the sprayed inhibitor covered area on the lid was estimated at 7.2 cm and the condensation rate of this area was calculated as 0.7 mL/(m<sup>2</sup>·s). For the specimen surface A1, as shown in Figure 16 (b), the condensation rate was higher than for the rest of the lid surface since it was directly cooled. The condensation rate on this part of the specimen was calculated at 1.4 mL/(m<sup>2</sup>·s). The C16-BDA inhibitor concentration in the condensed water droplets can be estimated based on a mass balance. Presuming that the concentration of CI in the condensed water was constant over time, the C16-BDA concentration in condensed water was calculated to be 72 ppm<sub>w</sub>. At room temperature (25°C), the solubility of C16-BDA in pure water is 50 ppm<sub>w</sub>. Consequently, it is reasonable to assume that 72 ppm<sub>w</sub> is close to the solubility limit of C16-BDA in the solution at the tested temperature (T<sub>specimen</sub>= 35.5°C).

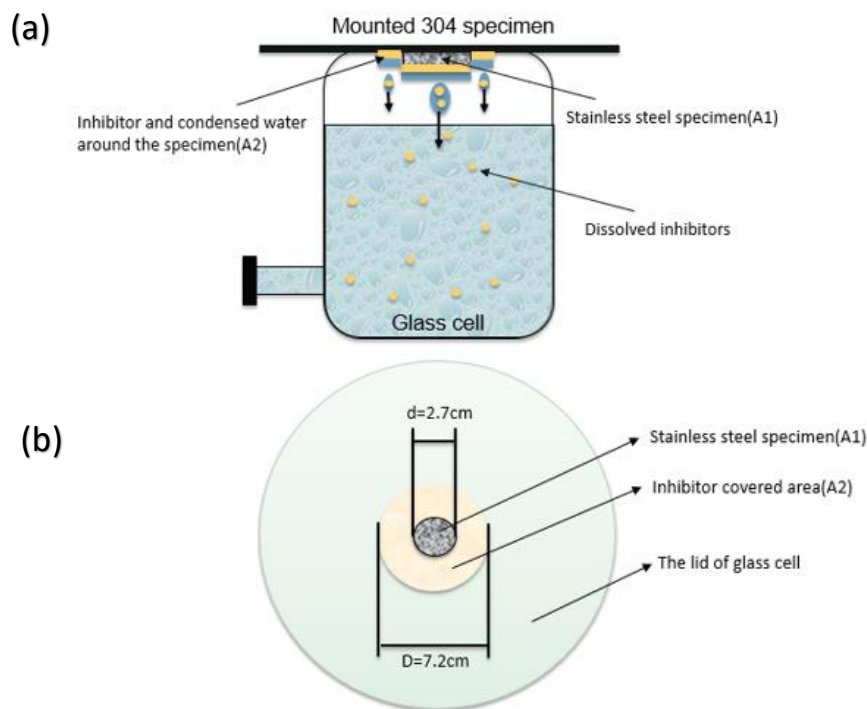


**Figure 16 Schematics of specimen characteristics related to CI concentration change with the exposure time: (a) inhibitor dissolving in condensed droplets from the specimen surface; (b) inhibitor sprayed area on the lid.**

Based on the mass balance between the inhibitor on the specimen surface and in the droplets, the concentration of the inhibitor present on the specimen surface and its change with the exposure time can be calculated knowing the concentration of C16-BDA in the condensed water. This is presented in Figure 17.

Figure 17 shows that the concentration of CI in the condensed water should be higher than its solubility limit (72ppm<sub>w</sub>) during the first 72 hours of exposure time – this is obviously impossible. Instead, it is hypothesized that, during that time, the inhibitor was present on the metal surface as a waxy solid in contact and in equilibrium with the condensed water, which maintained a CI concentration at the solubility limit (77 ppm<sub>w</sub>). As the condensation process proceeded, the CI waxy solid continuously dissolved in the condensed water until complete dissolution, which occurred approximately after 72

hours of exposure. This is represented in Figure 17, which shows the change in Cl concentration with time (yellow curve in Figure 17), which is corrected for the presence of the Cl waxy solid (red line in Figure 17). The figure shows that the inhibitor concentration on the condensed water should have remained at 77 ppm<sub>w</sub> for the first 77 hours of testing. It should then have decreased due to complete depletion of the Cl waxy solid. In this model, the corrosion inhibition should also be expected for up to 77 hours after the experiment started, i.e. as long as the Cl waxy solid was still present on the metal surface. In other words, based on this inhibitor concentration analysis, the inhibitor should have 77 hours of persistency, while the corrosion rate measurements based on the Fe<sup>2+</sup> concentration in condensed water showed that the persistency was only 30 hours. One possible explanation is that the amount of inhibitor that covered the specimen surface, applied by using the spraying method, was lower than expected due to the type of the spray nozzle and the configuration of the spraying assembly. Efforts are underway to address this discrepancy.

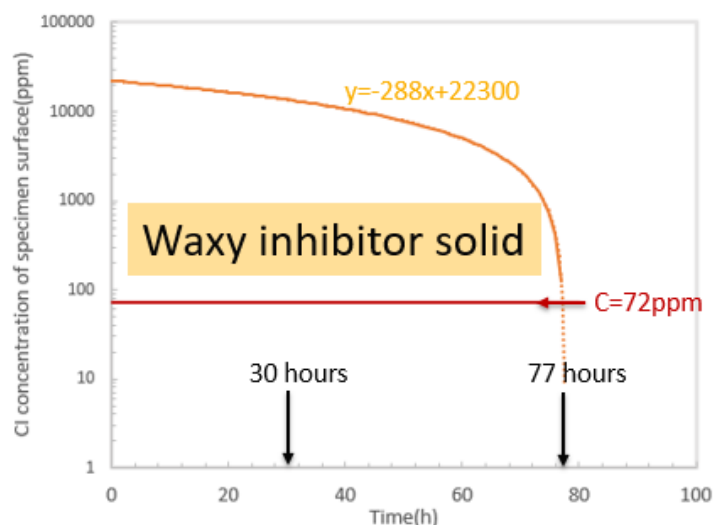


**Figure 17 Predicted inhibitor concentration of specimen surface change with time (the experimental conditions:  $T_{\text{gas}}$  65°C,  $T_{\text{specimen}}$  35.5°C,  $p\text{CO}_2$  0.65 bar, condensation rate 1.4 mL/(m<sup>2</sup>·s)).**

The experiments were also conducted under a lower condensation rate (0.48 mL/(m<sup>2</sup>·s)) and with a lower inhibitor concentration in the spraying solution (7.5wt% 1mL) to verify, at least qualitatively, the accuracy of the inhibitor concentration change (and persistency) model. Figure 18 shows the predicted change of inhibitor concentration on the specimen surface with time, in different experimental conditions. According to the calculations, the time required for the Cl waxy solid to reach full dissolution can be predicted. If the condensation rate is decreased to 0.48 mL/(m<sup>2</sup>·s), the waxy solid inhibitor persistency is naturally increased (from 72 to 96 hours). If the inhibitor concentration in the spraying solution is decreased (7.5wt% 1mL), the waxy solid inhibitor persistency is naturally decreased as well (from 72 to 37 hours). It is worth noticing that the corrosion rate measurements, based on the Fe<sup>2+</sup> concentration in condensed water, showed the same trend, although the persistency times were still quite different (16 and 38 hours compared to 37 and 96 hours, respectively). The reason for the discrepancy could be related, as mentioned earlier, to the spraying assembly and it still under investigation.

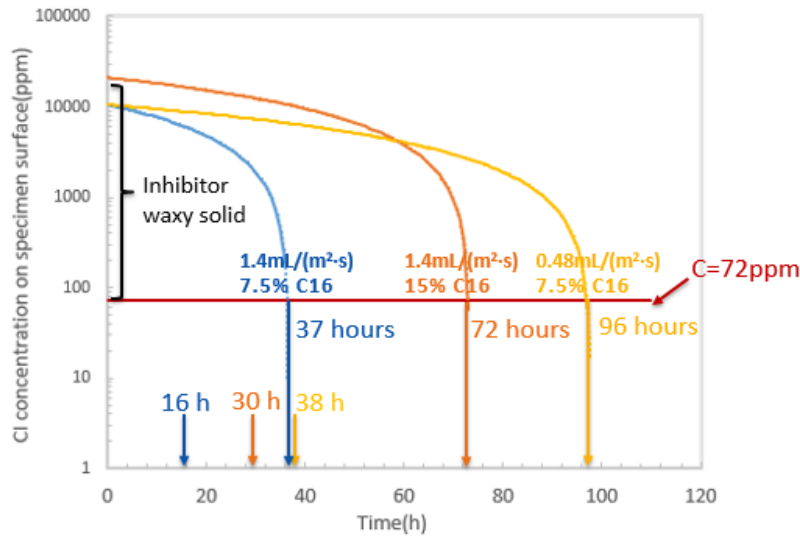


**Figure 18 Predicted inhibitor concentration of specimen surface vs time.**

## CONCLUSIONS

A BCI testing procedure that can maintain stable water chemistry, avoid O<sub>2</sub> contamination, and be adapted to TLC environments was developed. Testing and evaluation of a batch inhibitor for BLC and TLC mitigation was then performed. The pre-filming procedure and corrosion testing was done in the same glass cell. During the corrosion testing process, bottom of the line corrosion rate was measured via LPR and top of the line corrosion rates were characterizing using dissolved Fe<sup>2+</sup> concentration in the condensed water. UV-vis spectroscopy was applied to monitor corrosion inhibitor concentration. The following main conclusions on BLC and TLC scenarios were obtained:

### BLC

- The UV-vis measurement showed there was no inhibitor in the glass cell solution after it was rinsed 7 times, meaning that the proposed rinsing procedure could effectively remove all the inhibitor dissolved in the main electrolyte.
- At the beginning of the LPR measurements, there was no inhibitor in the glass cell except for the inhibitor film adsorbed on the specimen surface. The inhibitor concentration in the glass cell solution increased gradually with the exposure time due to its continuous desorption from the specimen surface.
- Continuous rinsing of the electrolyte during the experiments ensured the Cl concentration was kept at a minimum in the glass cell, thus maintaining stable water chemistry and avoiding the influence of desorbed inhibitor on corrosion rate measurement. Continuous rinsing could ensure that the Cl concentration stays at undetectable levels during the entire test duration.

### TLC

- The experimental setup with the inhibitor spray nozzle was successful in simulating BCI application to combat TLC.
- The inhibitor sprayed on the TLC specimen surface formed a waxy solid which gradually dissolved into the condensed water, and which was continuously transported to the bottom of the glass cell by falling droplets, leading to a diminution in corrosion resistance.
- The concentration of inhibitor in the condensed water was measured at 72 ppm<sub>w</sub> based on UV-vis measurement and the analysis of C16-BDA concentration in the bottom solution. This value is assumed to correspond to the Cl solubility limit in water in the tested conditions.

- The change in Cl concentration in the condensed water was modeled and persistency time could be predicted, giving trends qualitatively similar to what was measured with corrosion results. However, discrepancies between measured and predicted persistency times were noticed and could be related to the spraying assembly, which may have sprayed on the specimen surface a amount of Cl lower than expected. Efforts are underway to address this discrepancy.

### ACKNOWLEDGEMENTS

The author would like to thank the following companies for their financial support: MI-Swaco, PTTEP, Shell, Saudi Aramco, and Arkema. Also, much appreciated to the technical support from the lab's staff at the Institute for Corrosion and Multiphase Technology by Mr. Alexis Barxias and Mr. Cody Shafer.

### REFERENCES

- [1] H.H. Uhlig and W. R. Revie. "Corrosion and Corrosion Control: An Introduction to Corrosion Science and Engineering." John Wiley & Sons, Inc. (2008).
- [2] G. Koch, J. Varney and N. Thompson. "International Measures of Prevention, Application and Economics of Corrosion Technologies Study (IMPACT)." NACE International Report. (2016).
- [3] S. Netic, B.F.M. Pots, J. Postlethwaite, N. Thevenot, "Superposition of Diffusion and Chemical Reaction Controlled Limiting Currents—Application to CO<sub>2</sub> Corrosion," *Journal of Corrosion Science and Engineering*. 1, 3 (1995).
- [4] M. Nordsveen, S. Netic, R. Nyborg, A. Stangeland, "A Mechanistic Model for Carbon Dioxide Corrosion of Mild Steel in the Presence of Protective Iron Carbonate Films-Part 1: Theory and Verification," *Corrosion*. 59, 5 (2003): p. 443-456.
- [5] S. Netic, M. Nordsveen, R. Nyborg, A. Stangeland, "A Mechanistic Model for Carbon Dioxide Corrosion of Mild Steel in the Presence of Protective Iron Carbonate Films-Part 2: A Numerical Experiment," *Corrosion*. 59, 6 (2003): p. 489-497.
- [6] S. Netic, "Key Issues Related to Modelling of Internal Corrosion of Oil and Gas Pipelines-A Review," *Corrosion Science*. 49, 12 (2007): p. 4308-4338.
- [7] E. Remita, B. Tribollet, E. Sutter, V. Vivier, F. Ropital, J. Kittel, "Hydrogen Evolution in Aqueous Solutions Containing Dissolved CO<sub>2</sub>: Quantitative Contribution of the Buffering Effect," *Corrosion Science*. 50, 5 (2008): p. 1433-1440.
- [8] A. Kahyarian, B. Brown, S. Netic, "Electrochemistry of CO<sub>2</sub> Corrosion of Mild Steel: Effect of CO<sub>2</sub> on Iron Dissolution Reaction," *Corrosion Science*. 129, (2017): p. 146-151.
- [9] M. Finšgar and J. Jackson, "Application of Corrosion Inhibitors for Steels in Acidic Media for the Oil and Gas Industry: A Review," *Corrosion Science*. 86, (2014): p. 17-41.
- [10] J. Yang, V. Jovancicevic, S. Mancuso and J. Mitchell. "High performance batch treating corrosion inhibitor." NACE (2007) Nashville, Tennessee: paper no. 51300-07693-SG.
- [11] C. M Menendez, J M. Bojes, and J. Lerbscher. "Obtaining batch corrosion inhibitor film thickness measurements using an optical profiler." *Corrosion*. (2011); 67(3): p. 035003-1-035003-12.
- [12] R. De Marco, W. Durnie, A. Jefferson and B. Kinsella. "Persistence of carbon dioxide corrosion inhibitors." *Corrosion*. (2002); 58 (4): p. 354-363.
- [13] J.M. Dominguez Olivo, D. Young, B. Brown, S. Netic, "Effect of corrosion inhibitor alkyl tail length on the electrochemical process underlying CO<sub>2</sub> corrosion of mild steel," NACE Corrosion Conference (2018), Houston, TX, paper no.11537.
- [14] S. Netic, J. Postlethwaite and S. Olsen. An Electrochemical Model for Prediction of Corrosion of Mild Steel in Aqueous Carbon Dioxide Solutions. *Corrosion Science*. (1996): 0010-9312.
- [15] D. F. Swinehart. "The Beer-Lambert Law". *Journal of Chemical Education* 1962 39 (7), 333.